

**Genetic basis of a violation of Dollo's law: re-evolution of rotating sex combs in *Drosophila*
bipunctinata.**

Thaddeus Seher¹, Chen Siang Ng^{1,2}, Sarah Signor¹, Ondrej Podlaha^{1,3}, Olga Barmina¹, and
Artyom Kopp^{1*}

¹ Department of Evolution and Ecology, University of California – Davis, Davis CA 95616
USA

² Present address: Biodiversity Research Center, Academia Sinica, Taipei 11529, Taiwan

³ Present address: Department of Biostatistics and Computational Biology, Dana-Farber Cancer
Institute, and Department of Biostatistics, Harvard School of Public Health, Boston, MA 02115,
USA

Running title: *Genetics of Dollo's law*

Keywords: Dollo's law, sexual dimorphism, chromosomal inversions, morphological evolution,
QTL mapping

* Address for correspondence:

Artyom Kopp

Department of Evolution and Ecology

University of California – Davis

Davis, CA 95616 USA

akopp@ucdavis.edu

Author contributions:

TS performed transcriptome assembly, genotyping, and QTL mapping and co-wrote the paper

CSN performed genetic crosses and phenotypic analysis

SS performed genotyping

OP performed transcriptome sequencing

OB performed pyrosequencing assays

AK performed genetic crosses and chromosome squashes and co-wrote the paper

ABSTRACT

Phylogenetic analyses suggest that violations of “Dollo’s law” – that is, re-evolution of lost complex structures – do occur, albeit infrequently. However, the genetic basis of such reversals has not been examined. Here, we address this question using the *Drosophila* sex comb – a recently evolved, male-specific morphological structure composed of modified bristles. In some species, sex comb development involves only the modification of individual bristles, while other species have more complex “rotated” sex combs that are shaped by coordinated migration of epithelial tissues. Rotated sex combs were lost in the *ananassae* species subgroup and subsequently re-evolved, some 12 million years later, in *Drosophila bipectinata* and its sibling species. We examine the genetic basis of the differences in sex comb morphology between *D. bipectinata* and *D. malerkotliana*, a closely related species with a much simpler sex comb representing the ancestral condition. QTL mapping reveals that over 50% of this difference is controlled by one chromosomal inversion that covers approximately 5% of the genome. Several other, larger inversions do not contribute appreciably to the phenotype. This genetic architecture suggests that rotating sex combs may have re-evolved through changes in relatively few genes. We discuss potential developmental mechanisms that may allow lost complex structures to be regained.

INTRODUCTION

Dollo's "law of irreversibility" posits that complex morphological structures, once lost during evolution, cannot be regained in the same form. This principle makes intuitive sense: resurrecting an extinct developmental pathway in close to its ancestral condition seems biologically as well as statistically implausible. And yet, phylogenetic analyses have revealed several cases where Dollo's law is apparently violated. Examples include re-evolution of lost digits in lizards (BRANDLEY *et al.* 2008; KOHLSDORF *et al.* 2010; KOHLSDORF and WAGNER 2006), eggshells and oviparity in boas (LYNCH and WAGNER 2010), wings in stick insects (WHITING *et al.* 2003), shell coiling in limpets (COLLIN and CIPRIANI 2003), mandibular teeth in frogs (WIENS 2011), molars in lynx (KURTEN 1963), and others. There is a growing consensus that lost structures can sometimes be regained, especially if that happens soon after the initial loss (WIENS 2011) (but see (GALIS *et al.* 2010; GOLDBERG and IGIC 2008) for counter-arguments). This shifts the question from the realm of phylogenies to developmental genetics: *how* can complex structures re-evolve? What is the genetic basis of such reversals?

In this report, we examine the genetic basis of a likely violation of Dollo's law that occurred during the evolution of *Drosophila* sex combs. Sex combs are male-specific arrays of modified mechanosensory bristles ("teeth") that evolved within the genus *Drosophila* and are used by males during courtship and mating (KOPP 2011). These structures develop from either transverse or longitudinal bristle rows that are present on the front legs of both sexes, and show extensive morphological diversity but essentially fall into three distinct types. "Rotating" sex combs develop from one or several transverse bristle rows (TBRs) that undergo a 90 degree

rotation. This rotation is driven by a precisely coordinated rearrangement of several hundred epithelial cells that, assisted by strong homophilic adhesion between adjacent bristle cells, moves the embedded bristle rows from a transverse to a more longitudinal orientation (ATALLAH *et al.* 2009a; ATALLAH *et al.* 2009b; TANAKA *et al.* 2009). In contrast, “transverse” sex combs are simply TBRs composed of modified bristles. In this case, sex comb development is limited to the modification of individual bristle shafts and does not involve any morphogenetic movements (KOPP 2011). Finally, “longitudinal” sex combs resemble rotating sex combs in adult flies but actually develop from longitudinal bristle rows and are not homologous to the rotating sex combs on a cell-by-cell basis (ATALLAH *et al.* 2009b; TANAKA *et al.* 2009). Sex comb evolution presents many examples of divergence and convergence, and each developmental mechanism has evolved more than once (ATALLAH *et al.* 2009b; ATALLAH *et al.* 2012; TANAKA *et al.* 2009) (Figure 1A).

An apparent violation of Dollo’s law is observed in the *ananassae* subgroup of the *melanogaster* species group. This lineage consists of over 20 species, most of which have simple transverse sex combs (MATSUDA *et al.* 2009) (Figure 1 A, B). The only exception is found in one pair of sibling species, *D. bipectinata* and *D. parabipectinata*, which have much more dramatic sex combs that develop by active rotation (Figure 1 A, C). Detailed analysis of cell behavior during the pupal stage shows that this rotation occurs by the same mechanism as in distantly related groups such as the *obscura* species group and *D. melanogaster* and its relatives (ATALLAH *et al.* 2009b; TANAKA *et al.* 2009). *D. bipectinata* and *D. parabipectinata* branch deeply within the *ananassae* subgroup, while all basal lineages have transverse sex combs. Phylogenetic analysis strongly suggests that the common ancestor of these species has re-

evolved a rotating sex comb following a previous loss at the base of the *ananassae* subgroup (BARMINA and KOPP 2007; KOPP and BARMINA 2005; MATSUDA *et al.* 2009) (Figure 1 A).

D. bipectinata can be hybridized with its close relative *D. malerkotliana* (BOCK 1978; KOPP and BARMINA 2005), which has simple transverse sex combs, opening the way for a direct genetic analysis of sex comb re-evolution. We used a QTL mapping approach to identify the genomic regions responsible for the differences in sex comb morphology between *D. bipectinata* and *D. malerkotliana*. Surprisingly, we find that much of the species difference maps to a single chromosomal inversion that covers approximately 5% of the genome.

MATERIALS AND METHODS

***Drosophila* strains, crosses, and phenotypic analysis**

Drosophila strains were obtained from the US *Drosophila* Species Stock Center or provided by Drs. Y. Fuyama and M. Matsuda, and maintained on standard cornmeal media. Polytene chromosome spreads were prepared from salivary glands of female larvae using acetic orcein staining. Strains *D. malerkotliana* 14024-0391.00 and *D. bipectinata* 14024-0381.03 were inbred by single-pair, full-sib crosses for 12 and 18 generations, respectively, to generate derivative strains *mal0-sc2* and *bip3-isoA*. Interspecific hybridizations and subsequent crosses were performed in mass cultures, with at least 20 males and 20 females per generation. For phenotypic analysis, male legs were removed just above the tibia-tarsus joint, mounted in Hoyers media between two 60 x 22 mm coverslips, and examined under a high-power compound

microscope with brightfield illumination. Right and left legs from each male were kept together on an individual slide, and the average number of sex comb teeth per leg was recorded.

Transcriptome sequencing and identification of fixed differences between parental strains

To identify single nucleotide polymorphisms that distinguish *mal0-sc2* and *bip3-isoA*, normalized cDNA libraries were synthesized from whole-body adult RNA samples extracted from each strain. Paired-end libraries were prepared from the sheared, normalized cDNA using the standard Illumina protocol, and sequenced with 85-base paired-end reads on an Illumina Genome Analyzer II at the UC Davis Genome Center (Table S1). The partial transcriptomes of *mal0-sc2* and *bip3-isoA* were assembled *de novo* using ABySS (BIROL *et al.* 2009; MILLER *et al.* 2010; SIMPSON *et al.* 2009) followed by Trans-ABySS (ROBERTSON *et al.* 2010) and CAP3 (HUANG and MADAN 1999) (Table S2 and files S1A-B and S2A-B). For genetic analysis, we required fixed differences (FD) between parental strains, i. e. nucleotide positions where *bip3-isoA* is fixed for one allele and *mal0-sc2* for a different allele. To identify FDs for the first round of genotyping, *mal0-sc2* and *bip3-isoA* read libraries were each mapped separately to both *bip3-isoA* and *mal0-sc2* *de novo* transcriptome assemblies using SOAP2 (LI *et al.* 2009). Same-species mapping (*mal0-sc2* reads to *mal0-sc2* transcriptome and *bip3-isoA* reads to *bip3-isoA* transcriptome) serves to correct assembly errors, gauge coverage at each position, and identify nucleotide positions where multiple alleles segregate within each parental strain despite inbreeding. Cross-species mapping allows us to identify polymorphic positions and select FDs that meet coverage cut-offs. Transcriptome alignments yielded more than 40,000 FDs between *bip3-isoA* and *mal0-sc2* that are located in pairs of orthologous transcripts (file S3). For the

second round of genotyping, *bip3-isoA* and *mal0-sc2* cDNA reads were mapped to the *D. bipectinata* reference genome (GenBank AF000000000.1) (file S4). To identify the genomic locations of FDs, we BLASTed the sequence flanking each FD against the *D. ananassae* FlyBase 1.3 (July 2011) reference genome and transcriptome. The transcriptome assemblies and SNP datasets for *D. malerkotliana*, *D. bipectinata*, and several related species are described in detail in a separate publication (SIGNOR *et al.* submitted).

Genotyping and genetic mapping

To construct linkage maps and identify QTL intervals, we genotyped the progeny of two separate F₂ backcrosses and an F₃₈ introgression line (see Results). For the first round of genotyping, we selected 32 FDs that were evenly distributed among the major chromosome arms (Muller elements A-E) and were located at least 2.4Mb from each other in the *D. ananassae* genome (Table S3). Because the initial analysis suggested the presence of one or more strong QTLs on Muller E or proximal Muller D, we performed a second round of genotyping with 32 additional FDs concentrated on these chromosome arms. Genotyping primers were designed using Typer (Sequenom) based on the sequences of at least 70 bp upstream and 70 bp downstream from each candidate FD, after accounting for within-strain polymorphisms (Table S4). Individual flies were genotyped using MASSARRAY (Sequenom) single base extension in a 32-plex format using standard protocols (Table S5).

Linkage maps were constructed using R-QTL (BROMAN and SEN 2009; BROMAN *et al.* 2003). To map QTLs responsible for the differences in sex comb morphology, we applied the Haley-Knott, multiple imputation, and expectation-maximization models (DEMPSTER *et al.* 1977;

HALEY and KNOTT 1992; SEN and CHURCHILL 2001) to our data using the R-QTL package. All three methods gave nearly identical peak locations, LOD scores, and significance levels, indicating that the data are robust to over-parameterization. We first performed single-QTL scans to identify likely regions of genotype-phenotype association. For each detected QTL, we performed composite interval mapping and determined that genotypes at neighboring markers did not significantly affect the peak LOD score or width. We calculated the additive and epistatic interactions between all markers with scans utilizing two-QTL models. To determine the statistical significance of QTL peaks, we used a genome scan-adjusted P-value corresponding to the observed LOD score. The null distribution was derived through standard permutation test. To test for the presence of a QTL on the non-recombining 4th chromosome (Muller F), we genotyped two FDs in eight of the lightest and eight of the darkest individuals in each F₂ backcross using cleaved amplified polymorphism sequences (CAPS) (DARVASI and SOLLER 1992; KONIECZNY and AUSUBEL 1993). QTL association power analysis was performed using R-QTLDesign (SEN *et al.* 2006).

A more detailed description of sequencing and genotyping methods can be found in the Expanded Methods Section online (File S5).

Mapping candidate genes to the *D. bipectinata* genome

To determine the locations of *Scr* and *dsx* on our linkage maps, we BLASTed the full-length sequences of the *D. ananassae* genomic regions encompassing each gene, as well as the mature transcript of each gene, against the *D. bipectinata* genome assembly. Both the genomic and the transcript sequences mapped unambiguously to genome scaffolds that contained several

of our genotyping markers. *Scr* mapped to scaffold scf7180000396708, which also contained markers E-In(2L)D-u7 through E-In(2L)D-u13, while *dsx* mapped to scaffold scf7180000395971, which also contained marker E-In(2L)D-u16. On the linkage map, both of these scaffolds are located in the distal-most, non-recombining segment of Muller E (2L) corresponding to the inversion in In(2L)D. A similar BLAST analysis shows that genotyping markers linked to the major Muller E QTL are located in a different, more proximal non-recombining region corresponding to the inversion In(2L)M (Table S6).

Allele-specific expression analysis

Allele-specific pyrosequencing was performed in male F₁ hybrids between *D. bipunctinata* bip3-isoA and *D. malerkotliana* mal0-sc2. First and second pupal legs between 16 and 20 hours after pupariation were dissected and stored in TRIzol (Invitrogen) at -70°C. Three replicates of 24-43 individuals each were collected. RNA samples were extracted and reverse-transcribed using oligo(dT) primer and Superscript II (Invitrogen) following the manufacturer's protocols. Second strand synthesis was performed using DNA polymerase I and RNase-H. Nucleotide substitutions in the *Scr* sequence were identified by amplifying and sequencing a ~500 bp fragment of the second coding *Scr* exon from each parental strain. A 163 bp region flanking the chosen SNP was amplified using primers Fwd CATGTGGTACGGCACGATGTTCA and Rev biotin-GAGTTCCAATTCAACCGCTACCTG. Extension primer CTTGTGCTCCTTCTTCCAATTCA, which anneals upstream from the targeted SNP site, was used to measure allele-specific gene expression as described (WITTKOPP *et al.* 2004). The sequence immediately downstream of this primer is TAC in *D. bipunctinata* and TGC in *D. malerkotliana*. The polymorphic A/T site

corresponds to position 1871 in the *D. melanogaster Scr-A* transcript (Genbank accession number NM_079524).

RESULTS

Phenotypic and chromosomal variation in *D. bipectinata* and *D. malerkotliana*

To examine the genetics of re-evolution of large rotated sex combs, we carried out a series of crosses between *D. bipectinata* and *D. malerkotliana*. Prior to that analysis, we analyzed several strains of each species to estimate the degree of intraspecific variation. The number of sex comb teeth per leg varied from 5.2 ± 0.72 to 6.9 ± 1.03 in *D. malerkotliana* and from 13.6 ± 1.2 to 18.7 ± 1.37 in *D. bipectinata* (Table 1). There was no detectable variation in other aspects of sex comb morphology such as their position and orientation or the shape and color of teeth. Two strains of *D. bipectinata* and two of *D. malerkotliana* were crossed in all possible combinations and in both directions. F₁ hybrid males showed sex comb morphology that was intermediate in all respects (number of teeth, orientation, and tooth morphology and color). Males from reciprocal crosses showed only slight differences in sex comb size (Table S7), indicating that this phenotype is controlled predominantly by autosomal genes.

D. bipectinata and *D. malerkotliana* differ by several fixed chromosomal inversions, and each species is also polymorphic for many inversions (TOMIMURA *et al.* 2005). By examining the polytene chromosomes of multiple strains of each species and their F₁ hybrids, we determined that the strains *D. malerkotliana* 14024-0391.00 and *D. bipectinata* 14024-0381.03 differed by the smallest number of inversions, all but one of which are completely fixed between

the two species. The remaining inversion In(2L)D), which occupies the distal part of the chromosome arm 2L from 18A to 28D (Supplement table 8), is polymorphic within *D. bipectinata*. However, repeated attempts to cross the only available strain that lacked this inversion to different strains of *D. malerkotliana* did not succeed.

We inbred *D. malerkotliana* 14024-0391.00 and *D. bipectinata* 14024-0381.03 for 12 and 18 generations by single-pair full-sib crosses, respectively. The resulting strains, called *mal0-sc2* and *bip3-isoA*, were used for all subsequent experiments. These strains differ by one inversion each on XL and XR (Muller element A), two adjacent inversions on 2L (Muller E), none on 2R (Muller D), one on 3L (Muller C), and several overlapping inversions that cover almost the entire 3R (Muller B). The chromosome order of each strain is given in Table S8, and the autosomal inversions are shown in Figure S1. In crosses between these two strains, approximately 50% of the euchromatic genome is locked inside chromosomal inversions.

QTL mapping in F₂ hybrids identifies a major QTL on Muller-E

To estimate the number of genomic regions contributing to the dramatic difference in sex comb morphology between *D. bipectinata* and *D. malerkotliana*, we first performed two F₂ backcrosses between *mal0-sc2* and *bip3-isoA*. F₁ females from the cross between *D. malerkotliana* females and *D. bipectinata* males were crossed separately to *mal0-sc2* or *bip3-isoA* males. In the former cross, F₂ recombinant males are either heterozygous for the *D. malerkotliana* and *D. bipectinata* alleles, or homozygous for the *D. malerkotliana* allele at each locus; in the latter, F₂ males are either heterozygous or homozygous for the *D. bipectinata* alleles. We examined the sex combs of 427 and 528 F₂ males from these two crosses, respectively. In both panels, all

aspects of sex comb morphology were correlated: males with the largest number of sex comb teeth had fully rotated sex combs with curved dark teeth, males with the smallest number of teeth had unrotated sex combs with straight light teeth, and those with intermediate number of teeth were also intermediate in sex comb orientation and tooth morphology. The number of teeth could be quantified unambiguously, while the angle of rotation proved difficult to quantify due to the variation in the orientation of legs mounted on slides. We therefore used the number of teeth (average between the left and right forelegs) as proxy for species-specific sex comb morphology in subsequent analyses. The distribution of sex comb size in each F₂ backcross is shown in Figure 2 A, B.

188 F₂ males from the *mal0-sc2* backcross and 163 males from the *bip3-isoA* backcross were genotyped for 28 SNP markers distributed among all major chromosome arms. Since recombination was low and uneven due to inversion heterozygosity in F₁ females, linkage maps were inferred using a combination of empirical genetic distances and physical locations of the markers in the genomes of *D. bipectinata* and *D. ananassae* (Supplement figure 2). QTL analysis showed that, in both crosses, a large fraction of the difference between species was explained by a single genomic region that spanned most of Muller E (2L) (Figure 3). In the *mal0-sc2* backcross, mean sex comb size was 9.1 ± 1.12 for *malerkotliana* homozygotes and 12.3 ± 1.17 for *bipectinata/malerkotliana* heterozygotes for all markers on distal Muller E. In the *bip3-isoA* backcross, mean sex comb size was 14.2 ± 1.31 for *bipectinata/malerkotliana* heterozygotes and 17.2 ± 1.79 for *bipectinata* homozygotes. Thus, this QTL interval accounts for approximately 6 – 6.4 teeth, or slightly over 50% of the total difference between parental strains.

Other QTL intervals had much weaker effects. A QTL located on Muller C+B (3L+3R) was significant at the 95% level and had a total effect of ~1.43 teeth in the *D. malerkotliana* backcross, but was not significant with an effect of ~0.93 teeth in the *D. bipectinata* backcross (Figure 3). A possible QTL on Muller A (XL+XR) had an effect of ~0.98 teeth in the *D. bipectinata* backcross and ~0.65 teeth in the *D. malerkotliana* backcross, and did not reach significance in either panel. No QTLs were detected on Muller D (2R) or Muller F (the dot chromosome). Two-QTL scans did not reveal any epistatic interactions between the Muller E, Muller C+B, and Muller A QTLs, suggesting that the loci controlling variation in sex comb size act in an additive manner. Under the additive model, and assuming that both Muller C+B and Muller A contain true QTLs, all detected QTLs together explain only 7.9 – 8.4 teeth, or ~67-72% of the difference in sex comb size between *bip3-isoA* and *mal0-sc2*. The rest of this difference is likely to be controlled by even weaker QTLs that are below our power of detection. Assuming that all QTLs are fully additive, the number of genotyped males provides 95% power to detect a QTL with an effect size of at least 1.01 teeth in the *D. malerkotliana* backcross, or at least 1.41 teeth in the *D. bipectinata* backcross, for QTLs located on Muller A-E (LYNCH and WALSH 1998; SEN *et al.* 2007). These estimates are in agreement with the effect size of the weak QTL detected on Muller C+B.

Refined mapping localizes the major QTL to a single chromosomal inversion

The 2L/Muller E chromosome arm carries two adjacent interspecific inversions, In(2L)D (18A; 28D) and In(2L)M (28D; 34A) (Supplement table 8 and Supplement Figure 1). The proximal 2L (34A – 45D) and all of 2R/Muller D are free of inversions. To examine the genetic

basis of interspecific differences more closely, we sought to increase the amount of recombination between the *D. bipectinata* and *D. malerkotliana* genomes using an introgression approach. F₂ males were sterile in both backcrosses. We crossed F₂ females from the *mal0-sc2* backcross to *mal0-sc2* males. Some fraction of F₃ males were fertile when crossed to *mal0-sc2* females. In the F₄, we selected males with the largest sex combs, which were used to found an introgression strain. There is some recombination in *D. bipectinata* males but it is low compared to females (SINGH and BANERJEE 1996). Since the sex comb phenotype can only be scored in males, we used the following crossing scheme: in even-numbered generations, hybrid males with the largest sex combs were selected and crossed to *mal0-sc2* females, while in odd-numbered generations randomly chosen hybrid females were crossed to *mal0-sc2* males (Figure 4A). These crosses should eventually make the introgression strain homozygous for *D. malerkotliana* alleles at all loci, with the exception of genomic regions that are strongly linked to genes responsible for the interspecific differences in sex comb morphology.

We examined polytene chromosomes in the introgression strain after 20 generations. We found that it was polymorphic for In(2L)D and In(2L)M, indicating that it was heterozygous for the *D. bipectinata* and *D. malerkotliana* alleles on Muller E. On all other chromosome arms, the introgression was homozygous for the *D. malerkotliana* arrangement. This result suggested that only the 2L (and potentially 2R) made a major contribution to species differences, confirming the results of F₂ QTL mapping. Throughout the introgression process, different aspects of sex comb morphology (orientation and the number, shape, and color of teeth) continued to be correlated (Figure 4B).

After 36 total generations of introgression (corresponding to 19 recombining female generations), males with the largest sex combs were crossed to *mal0-sc2* females and the

resulting F₃₇ males and females were crossed to each other *en masse*. This resulted in F₃₈ males that could in principle be homozygous for the *D. bipectinata* allele, heterozygous, or homozygous for the *D. malerkotliana* allele at any locus. We examined the sex combs of 590 F₃₈ males. The distribution of sex comb sizes was more clearly bimodal than in the F₂ (Figure 2C), suggesting that this phenotype was largely controlled by a single genomic region and that some of the weaker QTLs have been removed by repeated back-crossing. 185 F₃₈ males were first genotyped for the same 28 SNP markers as the F₂ panels; preliminary QTL mapping was consistent with the F₂ results. We therefore genotyped the F₃₈ panel for 25 additional markers on Muller E and 6 additional markers on Muller D.

In the F₃₈ recombinant panel, all marker loci located on the proximal Muller E, most of Muller D, and all other chromosome arms were homozygous for *D. malerkotliana* alleles, while the distal portion of Muller E that carries the inversions In(2L)D and In(2L)M was polymorphic for the *D. bipectinata* and *D. malerkotliana* alleles and showed a strong association with the sex comb phenotype (Figure 5). We did not observe any males homozygous for the *D. bipectinata* alleles on Muller E, suggesting that some interaction between one or more *D. bipectinata* genes in this region with homozygous *D. malerkotliana* alleles elsewhere in the genome results in hybrid lethality. With a single exception (see below), the entire distal region of Muller E segregated as a single block, as expected from the inversion heterozygosity. Males homozygous for the *D. malerkotliana* alleles throughout this region had small sex combs, (8.3 ± 1.13 teeth), whereas the *malerkotliana* / *bipectinata* heterozygotes had sex combs that were intermediate in size between the parental species (11.3 ± 1.04) (Figure 5C). Thus, in the F₃₈ as well as in the F₂, this single QTL region accounts for ~6 teeth, slightly over 50% of the total difference between the *D. bipectinata* and *D. malerkotliana* parents. Sex comb size in the F₃₈ males homozygous for

the *D. malerkotliana* Muller E (8.3 ± 1.13 teeth) is larger than in the *mal0-sc2* parent (7.13 ± 1.13 teeth) but smaller than in the F₂ males homozygous for the *D. malerkotliana* Muller E (9.1 ± 1.12 teeth). This suggests that some of the minor QTLs persist in the introgression strain but are below our power of detection.

We observed a single recombination event between In(2L)D and In(2L)M. This rarity is not surprising given the close proximity between the inversion breakpoints. This fortuitous event allowed us to localize the region responsible for the differences in sex comb morphology more precisely. The recombinant male was homozygous for *D. malerkotliana* alleles in the more proximal block of markers, presumably corresponding to In(2L)M, but heterozygous for the *D. bipectinata* and *D. malerkotliana* alleles in the more distal block that presumably corresponds to In(2L)D (Figure 5C). The number of sex comb teeth in this male (8) almost exactly matches the mean sex comb size of the 93 males that are homozygous for *D. malerkotliana* alleles over the entire Muller E (8.30 teeth), but is clearly different from the mean phenotype of the 91 males that are heterozygous for the *D. bipectinata* and *D. malerkotliana* alleles in both In(2L)D and In(2L)M (11.32 teeth). This indicates that the major Muller E QTL interval corresponds to the In(2L)M inversion.

The markers that co-segregate with In(2L)M map to four scaffolds in the genome of *D. bipectinata*. Together, these scaffolds cover 6,049 kb and contain several hundred genes including transcription factors, Polycomb and Trithorax group genes, and other regulatory genes that could potentially affect sex comb development (Supplement Table 9). Since recombination mapping within the In(2L)M inversion is not feasible, we cannot determine whether this QTL corresponds to a single locus, or reflects the cumulative effect of several weaker QTLs.

***Scr* and *dsx* are not directly responsible for the interspecific differences.**

The HOX gene *Sex combs reduced* (*Scr*) and the sex determination gene *doublesex* (*dsx*) play central roles in sex comb development. The evolutionary origin of sex combs coincides with the origin of a new *dsx* expression domain and novel regulatory interactions between *Scr* and *dsx* (BARMINA and KOPP 2007; TANAKA *et al.* 2011). A combination of experimental and comparative evidence suggests that changes in *dsx* and *Scr* expression were responsible for sex comb evolution (KOPP 2011; TANAKA *et al.* 2011). Moreover, *dsx* and *Scr* expression differs between *D. bipectinata* and *D. malerkotliana* in a way consistent with their morphological differences (BARMINA and KOPP 2007; TANAKA *et al.* 2011). Since both genes are located on Muller E (2L of *D. bipectinata*), we tested whether they could be responsible for the differences in sex comb morphology between these species.

We used allele-specific pyrosequencing (COWLES *et al.* 2002; WITTKOPP *et al.* 2004) in F₁ hybrids between *bip3-isoA* and *mal0-sc2* to test whether the interspecific differences in *Scr* expression had a *cis*-regulatory component. We found that the *D. bipectinata* allele of *Scr* was expressed at a significantly higher level than the *D. malerkotliana* allele in the prothoracic, but not in the mesothoracic, pupal legs of F₁ hybrid males (t-test $P = 0.0003$; Figure 6). Thus, *Scr* expression has diverged between *D. malerkotliana* and *D. bipectinata* due at least in part to changes at the *Scr* locus.

To localize *Scr* and *dsx* relative to the linkage map and inversion boundaries, we Blasted the coding sequences of these genes and the transcriptome contigs that contained our genotyping markers against the *D. bipectinata* genome scaffolds. We found that both genes were located on genomic scaffolds that also included SNP markers that were part of the In(2L)D linkage block

(Figure 5, Table S6). In contrast, phenotypic differences between *D. malerkotliana* and *D. bipectinata* are associated with the In(2L)M block (Figure 5C). Thus, despite the evidence for *cis*-regulatory divergence at the *Scr* locus, neither that gene nor *dsx* are directly responsible for species divergence.

DISCUSSION

A single inversion, In(2L)M, is responsible for slightly more than half of the difference in sex comb morphology between *D. bipectinata* and *D. malerkotliana*. Minor QTLs located elsewhere in the genome have much weaker effects. In(2L)M spans chromosomal bands 28D – 34A, out of the total of 100 chromosome divisions. In other words, much of the interspecific difference maps to approximately 5% of the genome. Other chromosomal inversions that are also completely fixed between *D. malerkotliana* and *D. bipectinata*, including several inversions that are much larger than In(2L)M, make little or no contribution to the differences in sex comb morphology. Thus, although we cannot determine the number of genes in the In(2L)M inversion that contribute to its total effect, it is possible that this number is relatively small.

Re-evolution of large rotating sex combs in the last common ancestor of *D. bipectinata* and *D. parabiptinata* represents a major developmental change. The number of bristles recruited into the sex comb, rotation of the surrounding epithelium, the shape of bristle shafts, and their pigmentation have very different molecular underpinnings (KOPP 2011). Epithelial rotation in particular is a complex morphogenetic process involving localized convergent extension, and must require numerous genes involved in cell polarity, cell adhesion, and cytoskeletal dynamics (ATALLAH *et al.* 2009a; TANAKA *et al.* 2009). What types of genetic

changes could allow this entire suite of processes to re-evolve following an earlier loss (BARMINA and KOPP 2007; MATSUDA *et al.* 2009)?

We suggest that violations of Dollo's law can be made more likely by the modular organization of developmental pathways. Many pathways have "nexus" regulatory genes that activate multiple downstream targets responsible for different cellular processes. The loss of a complex trait can happen easily if the expression of the nexus gene in the progenitor tissue is disrupted, since the entire downstream developmental program will be lost automatically. In fact, rapid loss of morphological structures by loss-of-function mutations in a single regulatory gene has been documented in several cases (CHAN *et al.* 2009; MCGREGOR *et al.* 2007). The same property of developmental pathways could also explain the re-evolution of lost traits: as long as the downstream pathway remains intact, regaining the expression of the nexus gene or genes in the progenitor tissue will be sufficient to restore much of the original structure. For example, several lineages of swordtail fish (*Xiphophorus*) have secondarily lost the male swords (extended tail fins) (MEYER *et al.* 1994; MEYER *et al.* 2006). In at least some of these species, small vestigial "swordlets" can be restored by exposure to abnormally high levels of testosterone (GORDON *et al.* 1943). In *X. maculatus*, a swordless species, a single mutation is sufficient to form a similar (though not identical) fin extension, presumably by enhancing cell response to endogenous testosterone (OFFEN *et al.* 2008). These observations suggest that the pathway responsible for sword development has decayed only partially following the loss of the sword, and can be brought back by changes in a relatively small number of genes. On a much deeper timescale, teeth are absent in all modern birds; however, a single mutation in the chicken *talpid2* gene can partially restore tooth development, inducing integumentary outgrowths that resemble crocodilian teeth (HARRIS *et al.* 2006). Of course, this is only possible because some of the

regulatory landscape that controls odontogenesis has been retained in avian oral tissues (CHEN *et al.* 2000; MITSIADIS *et al.* 2006).

The question, then, is why the downstream pathway (i. e., a large set of regulatory interactions among genes) would stay intact and not succumb to mutation accumulation in the absence of selection on the defunct structure. One possible explanation is that the vast majority of genes have pleiotropic functions. In the simplest case, the coding sequence of a gene whose expression has been lost in one tissue will remain under purifying selection as long as it continues to be expressed in other tissues (COLLIN and MIGLIETTA 2008; MARSHALL *et al.* 1994). More generally, the modular organization of development suggests that pleiotropy can protect entire pathways: selection pressure on most regulatory interactions may still be present if the pathway acts in other tissues. This mechanism may be particularly important for structures that have serial homologues, which share largely the same developmental programs. For example, re-evolution of lost digits in lizards and mandibular teeth in frogs is likely to be enabled by the fact that other digits, and other teeth, have always been retained (BRANDLEY *et al.* 2008; KOHLSDORF *et al.* 2010; WIENS 2011).

Even if selection does not preserve the entire pathway, preservation of its component modules may be enough to retain capacity for re-evolution. In *Drosophila*, the cellular module responsible for making thickened, rounded, darkly pigmented sex comb teeth may also be deployed to make similar bristles in other body parts such as male genitalia; the module responsible for sex comb rotation may act in other epithelial sheets that undergo convergent extension; and so on. If selection on pleiotropically linked traits preserves most regulatory interactions from mutational decay, the pathway as a whole could remain largely intact and require changes in only a few genes to restore it to a modestly functional state that can then be

refined by additional mutations. The genetic architecture of sex comb morphology in *D. bipectinata* versus *D. malerkotliana* could conceivably be the result of such process.

Understanding the molecular mechanisms that enable re-evolution of complex traits will require a developmental-genetic perspective; QTL mapping is only the first step in this direction. Although the limitations imposed by fixed chromosomal inversions preclude us from identifying the major gene or genes responsible for the re-evolution of large rotating sex combs in *D. bipectinata* by linkage mapping, our growing understanding of sex comb development may ultimately allow us to overcome these limitations.

ACKNOWLEDGEMENTS

We are grateful to Dr. Muneo Matsuda for his help in analyzing chromosome order in the *bipectinata* species complex, to Dr. Y. Fuyama and the San Diego *Drosophila* Species Stock Center for providing fly strains, and to Rachael Curtis, Andrew Hamilton, and Mary Magsombol for help with phenotypic analysis and DNA extractions. Illumina sequencing was performed at the UC Davis Genome Center. Genotyping was performed at the UC Davis Veterinary Genetics Laboratory. This work was supported by NIH grant 5-R01GM082843-02.

TABLES

Table 1. Sex comb size in three species of the *biplectinata* species complex.

SPECIES	STRAIN	NUMBER OF SEX COMB TEETH (mean \pm stdev)	N
<i>D. malerkotliana</i>	14024-0391.00	6.85 \pm 1.03	53
<i>D. malerkotliana</i>	SWB17	5.24 \pm 0.72	37
<i>D. biplectinata</i>	14024-0381.00	14.10 \pm 1.14	59
<i>D. biplectinata</i>	14024-0381.02	13.55 \pm 1.2	43
<i>D. biplectinata</i>	14024-0381.03	18.69 \pm 1.37	46
<i>D. biplectinata</i>	14024-0381.04	16.81 \pm 1.49	31
<i>D. parabipectinata</i>	14024-0401.00	12.38 \pm 1.08	40
<i>D. parabipectinata</i>	14024-0401.02	12.98 \pm 1.38	52

REFERENCES

- ATALLAH, J., N. H. LIU, P. DENNIS, A. HON, D. GODT *et al.*, 2009a Cell dynamics and developmental bias in the ontogeny of a complex sexually dimorphic trait in *Drosophila melanogaster*. *Evol Dev* **11**: 191-204.
- ATALLAH, J., N. H. LIU, P. DENNIS, A. HON and E. W. LARSEN, 2009b Developmental constraints and convergent evolution in *Drosophila* sex comb formation. *Evol Dev* **11**: 205-218.
- ATALLAH, J., H. WATABE and A. KOPP, 2012 Many ways to make a novel structure: Different mechanisms of sex comb development in *Lordiphosa* and *Sophophora*. *Evol Dev* (**in press**).
- BARMINA, O., and A. KOPP, 2007 Sex-specific expression of a HOX gene associated with rapid morphological evolution. *Dev Biol* **311**: 277-286.
- BIROL, I., S. D. JACKMAN, C. B. NIELSEN, J. Q. QIAN, R. VARHOL *et al.*, 2009 De novo transcriptome assembly with ABySS. *Bioinformatics* **25**: 2872-2877.
- BOCK, I. R., 1978 The bipectinata complex: A study of interspecific hybridization in the genus *Drosophila*. *Aust. J. biol. Sci.* **31**: 197--208.
- BRANDLEY, M. C., J. P. HUELSENBECK and J. J. WIENS, 2008 Rates and patterns in the evolution of snake-like body form in squamate reptiles: evidence for repeated re-evolution of lost digits and long-term persistence of intermediate body forms. *Evolution* **62**: 2042-2064.
- BROMAN, K. W., and Ś. SEN, 2009 *A Guide to QTL Mapping with R/qtl*. Springer, New York.
- BROMAN, K. W., H. WU, Ś. SEN and G. A. CHURCHILL, 2003 R/qtl: QTL mapping in experimental crosses. *Bioinformatics* **19**: 889-890.
- CHAN, Y. F., M. E. MARKS, F. C. JONES, G. VILLARREAL, JR., M. D. SHAPIRO *et al.*, 2009 Adaptive Evolution of Pelvic Reduction in Sticklebacks by Recurrent Deletion of a Pitx1 Enhancer. *Science*.
- CHEN, Y., Y. ZHANG, T. X. JIANG, A. J. BARLOW, T. R. ST AMAND *et al.*, 2000 Conservation of early odontogenic signaling pathways in Aves. *Proc Natl Acad Sci U S A* **97**: 10044-10049.
- COLLIN, R., and R. CIPRIANI, 2003 Dollo's law and the re-evolution of shell coiling. *Proc Biol Sci* **270**: 2551-2555.
- COLLIN, R., and M. P. MIGLIETTA, 2008 Reversing opinions on Dollo's Law. *Trends Ecol Evol* **23**: 602-609.
- COWLES, C. R., J. N. HIRSCHHORN, D. ALTSHULER and E. S. LANDER, 2002 Detection of regulatory variation in mouse genes. *Nat Genet* **32**: 432-437.
- DARVASI, A., and M. SOLLER, 1992 Selective genotyping for determination of linkage between a marker locus and a quantitative trait locus. *TAG Theoretical and Applied Genetics* **85**: 353-359.
- DEMPSTER, A. P., N. M. LAIRD and D. B. RUBIN, 1977 Maximum Likelihood from Incomplete Data via the EM Algorithm (with discussion). *Journal of the Royal Statistical Society. Series B (Methodological)* **39**: 1-38.
- GALIS, F., J. W. ARNTZEN and R. LANDE, 2010 Dollo's law and the irreversibility of digit loss in *Bachia*. *Evolution* **64**: 2466-2476; discussion 2477-2485.
- GOLDBERG, E. E., and B. IGIC, 2008 On phylogenetic tests of irreversible evolution. *Evolution* **62**: 2727-2741.

- GORDON, M., H. COHEN and R. NIGRELLI, 1943 A Hormone-Produced Taxonomic Character in *Platyopocilus maculatus* Diagnostic of Wild *P. xiphidium*. *American Naturalist* **77**: 569-572.
- HALEY, C. S., and S. A. KNOTT, 1992 A simple regression method for mapping quantitative trait loci in line crosses using flanking markers. *Heredity* **69**: 315-324.
- HARRIS, M. P., S. M. HASSO, M. W. FERGUSON and J. F. FALLON, 2006 The development of archosaurian first-generation teeth in a chicken mutant. *Curr Biol* **16**: 371-377.
- HUANG, X., and A. MADAN, 1999 CAP3: A DNA Sequence Assembly Program. *Genome Research* **9**: 868-877.
- KOHLSDORF, T., V. J. LYNCH, M. T. RODRIGUES, M. C. BRANDLEY and G. P. WAGNER, 2010 Data and data-interpretation in the study of limb evolution: a reply to Galis et al., on the re-evolution of digits in the lizard genus *Bachia*. *Evolution* **64**: 2477-2485.
- KOHLSDORF, T., and G. P. WAGNER, 2006 Evidence for the reversibility of digit loss: a phylogenetic study of limb evolution in *Bachia* (Gymnophthalmidae: Squamata). *Evolution* **60**: 1896-1912.
- KONIECZNY, A., and F. M. AUSUBEL, 1993 A procedure for mapping *Arabidopsis* mutations using co-dominant ecotype-specific PCR-based markers. *The Plant Journal* **4**: 403-410.
- KOPP, A., 2011 *Drosophila* Sex Combs as a Model of Evolutionary Innovations. *Evol Dev* **in press**.
- KOPP, A., and O. BARMINA, 2005 Evolutionary history of the *Drosophila* *biplectinata* species complex. *Genet Res* **85**: 23-46.
- KURTEN, B., 1963 Return of a lost structure in the evolution of the felid dentition. *Comment. Biol.* **26**: 1-12.
- LI, R., C. YU, Y. LI, T.-W. LAM, S.-M. YIU *et al.*, 2009 SOAP2: an improved ultrafast tool for short read alignment. *Bioinformatics* **25**: 1966-1967.
- LYNCH, M., and B. WALSH, 1998 *Genetics and analysis of quantitative traits*. Sinauer, Sunderland, Mass.
- LYNCH, V. J., and G. P. WAGNER, 2010 Did egg-laying boas break Dollo's law? Phylogenetic evidence for reversal to oviparity in sand boas (*Eryx*: Boidae). *Evolution* **64**: 207-216.
- MARSHALL, C. R., E. C. RAFF and R. A. RAFF, 1994 Dollo's law and the death and resurrection of genes. *Proc Natl Acad Sci U S A* **91**: 12283-12287.
- MATSUDA, M., C.-S. NG, M. DOI, A. KOPP and Y. N. TOBARI, 2009 Evolution in the *Drosophila* *ananassae* species subgroup. *Fly* **3**: 1-13.
- MCGREGOR, A. P., V. ORGOGOZO, I. DELON, J. ZANET, D. G. SRINIVASAN *et al.*, 2007 Morphological evolution through multiple cis-regulatory mutations at a single gene. *Nature* **448**: 587-590.
- MEYER, A., J. M. MORRISSEY and M. SCHARTL, 1994 Recurrent origin of a sexually selected trait in *Xiphophorus* fishes inferred from a molecular phylogeny. *Nature* **368**: 539-542.
- MEYER, A., W. SALZBURGER and M. SCHARTL, 2006 Hybrid origin of a swordtail species (Teleostei: *Xiphophorus clemenciae*) driven by sexual selection. *Mol Ecol* **15**: 721-730.
- MILLER, J. R., S. KOREN and G. SUTTON, 2010 Assembly algorithms for next-generation sequencing data. *Genomics* **95**: 315-327.
- MITSIADIS, T. A., J. CATON and M. COBOURNE, 2006 Waking-up the sleeping beauty: recovery of the ancestral bird odontogenic program. *J Exp Zool B Mol Dev Evol* **306**: 227-233.
- OFFEN, N., N. BLUM, A. MEYER and G. BEGEMANN, 2008 *Fgfr1* signalling in the development of a sexually selected trait in vertebrates, the sword of swordtail fish. *BMC Dev Biol* **8**: 98.

- ROBERTSON, G., J. SCHEIN, R. CHIU, R. CORBETT, M. FIELD *et al.*, 2010 De novo assembly and analysis of RNA-seq data. *Nat Meth* **7**: 909-912.
- SEN, S., and G. A. CHURCHILL, 2001 A Statistical Framework for Quantitative Trait Mapping. *Genetics* **159**: 371-387.
- SEN, S., J. SATAGOPAN, K. W. BROMAN and G. A. CHURCHILL, 2006 R/qtlDesign: Inbred Line Cross Experimental Design, pp.
- SEN, S., J. M. SATAGOPAN, K. W. BROMAN and G. A. CHURCHILL, 2007 R/qtlDesign: inbred line cross experimental design. *Mamm Genome* **18**: 87-93.
- SIGNOR, S. A., T. D. SEHER and A. KOPP, submitted Genomic resources for multiple species in the *Drosophila ananassae* species group. *Fly (Austin)*.
- SIMPSON, J. T., K. WONG, S. D. JACKMAN, J. E. SCHEIN, S. J. JONES *et al.*, 2009 ABySS: a parallel assembler for short read sequence data. *Genome Res* **19**: 1117-1123.
- SINGH, B. N., and R. BANERJEE, 1996 Spontaneous recombination in males of *Drosophila bipectinata*. *J. Biosci., Bangalore* **21**: 775--779.
- TANAKA, K., O. BARMINA and A. KOPP, 2009 Distinct developmental mechanisms underlie the evolutionary diversification of *Drosophila* sex combs. *Proc Natl Acad Sci U S A* **106**: 4764-4769.
- TANAKA, K., O. BARMINA, L. E. SANDERS, M. N. ARBEITMAN and A. KOPP, 2011 Evolution of Sex-Specific Traits through Changes in HOX-Dependent doublesex Expression. *PLoS Biol* **9**: e1001131.
- TOMIMURA, Y., M. MATSUDA and Y. N. TOBARI, 2005 Chromosomal phylogeny and geographical divergence in the *Drosophila bipectinata* complex. *Genome* **48**: 487-502.
- WHITING, M. F., S. BRADLER and T. MAXWELL, 2003 Loss and recovery of wings in stick insects. *Nature* **421**: 264-267.
- WIENS, J. J., 2011 Re-evolution of lost mandibular teeth in frogs after more than 200 million years, and re-evaluating Dollo's law. *Evolution* **65**: 1283-1296.
- WITTKOPP, P. J., B. K. HAERUM and A. G. CLARK, 2004 Evolutionary changes in cis and trans gene regulation. *Nature* **430**: 85-88.

FIGURE LEGENDS

Figure 1. Re-evolution of rotating sex combs in *D. bipectinata*. **A.** A simplified phylogenetic tree showing the position of *D. bipectinata* and its relatives. Black indicates a rotated (longitudinal) sex comb, grey a transverse sex comb, and white a primitively absent sex comb. The striped triangle shows a lineage where species have either rotated or transverse sex comb. In the *ficuspshila* and *montium* subgroups, sex combs develop from longitudinal bristle rows and do not undergo active rotations. The *obscura* species group, the Oriental subgroups, and *D. bipectinata* and *D. parabipectinata* have actively rotating sex combs (KOPP 2011). Some

species in the subgenus *Lordiphosa* also have actively rotating sex combs (ATALLAH *et al.* 2012). The most likely evolutionary scenario is that actively rotating sex combs were present in the last common ancestor of the *melanogaster* and *obscura* species group, were lost at the base of the *ananassae* subgroup, and re-evolved in the last common ancestor of *D. bipectinata* and *D. parabiptinata* (MATSUDA *et al.* 2009). **B.** The sex comb of *D. malerkotliana*. **C.** The sex comb of *D. bipectinata*.

Figure 2. Distribution of sex comb size in the genotyping panels. **A.** Progeny of *D. malerkotliana* mal0-sc2 / *D. bipectinata* bip3-isoA F₁ hybrid females and bip3-isoA males. **B.** Progeny of *D. malerkotliana* mal0-sc2 / *D. bipectinata* bip3-isoA F₁ females and mal0-sc2 males. **C.** F₃₈ introgression (see text for details).

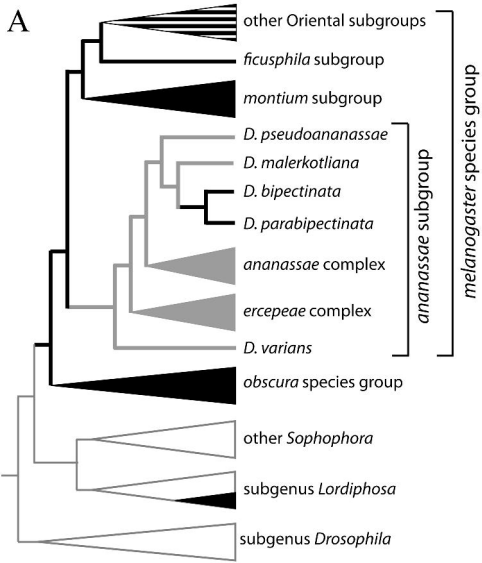
Figure 3. QTL mapping of sex comb size in the F₂ backcrosses. **A.** The progeny of *D. malerkotliana* mal0-sc2 / *D. bipectinata* bip3-isoA F₁ females and mal0-sc2 males. **B.** Progeny of *D. malerkotliana* mal0-sc2 / *D. bipectinata* bip3-isoA F₁ hybrid females and bip3-isoA males. The genome-wide significance threshold is 2.27 in the former cross and 2.72 in the latter. The X axis is in centimorgans. Marker names and locations are indicated as follows. Each marker name begins with the Muller element on which it is located and ends with the arbitrary marker number. For markers inferred to be inside a chromosomal inversion, the name of that inversion is added in the middle. Since these and adjacent markers co-segregated as non-recombining blocks, their relative positions could not be determined by meiotic mapping. The numbers of such markers are preceded by “u” for “unmapped” and their order on the map is arbitrary. For example, E-In(2L)D-u4 is marker #4 located on Muller E (chromosome arm 2L) in the inversion

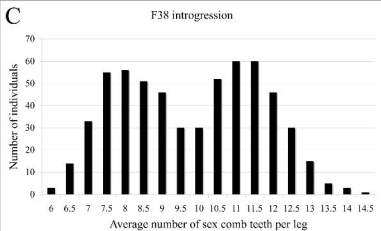
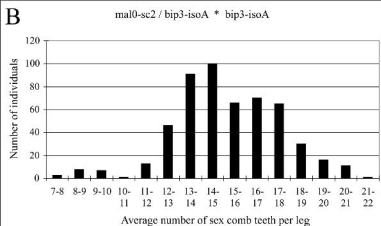
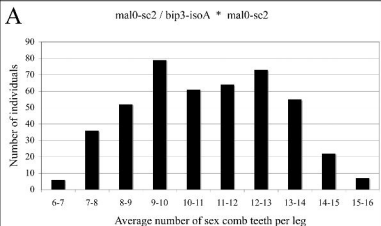
In(2L)D and could not be mapped by recombination, while D-3 is marker #3 located on Muller D (chromosome arm 2R) outside of any inversions.

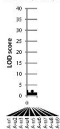
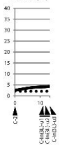
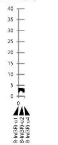
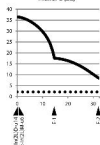
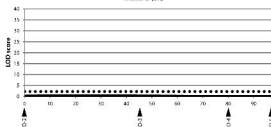
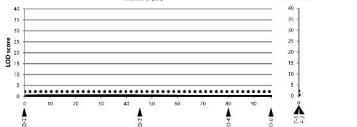
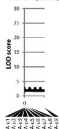
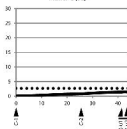
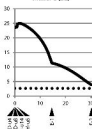
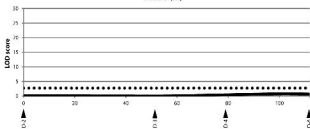
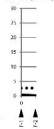
Figure 4. Phenotypic introgression between *D. bipectinata* and *D. malerkotliana*. **A.** Crossing scheme. **B.** Sex comb of a male from the introgression strain after >20 generations of back-crossing.

Figure 5. QTL mapping of sex comb size in the introgression line. **A.** QTL plot. Markers genotyped in both the F₂ and the introgression are highlighted in bold; markers that were only genotyped in the introgression are in plain font. Markers and candidate genes located on the same scaffold in the genome sequence of *D. bipectinata* are connected by horizontal lines at the top. See legends to Figure 3 and Supplement Figure 2 for marker nomenclature. **B.** Locations of genotyping markers and candidate genes relative to chromosomal inversions. Note that most markers could not be mapped by recombination because they either are located inside inversions (In(2L)D and In(2L)M) or were homozygous for *D. malerkotliana* alleles. Markers that were mapped by recombination in the F₂ are shown above the line. **C.** Phenotypes associated with different haplotype blocks. Light grey shows markers that were homozygous for the *D. malerkotliana* allele, and dark grey indicates the markers that were heterozygous for the *D. malerkotliana* and *D. bipectinata* alleles.

Figure 6. Allele-specific expression of *Scr* in the F₁ hybrids between *D. bipectinata* bip3-isoA and *D. malerkotliana* mal0-sc2. The Y axis shows the proportion of overall expression represented by each species-specific allele. Error bars are based on three biological replicates.





A**Muller A (XL+XR)****Muller C (3L)****Muller B (3R)****Muller E (2L)****Muller D (2R)****Muller F (4L+4R)****B****Muller A (XL+XR)****Muller C (3L)****Muller B (3R)****Muller E (2L)****Muller D (2R)****Muller F (4R+4L)**

A

♀ *bipectinata* × ♂ *malerkotliana*

(recombination)
♀ **hybrid** × ♂ *malerkotliana*

Select males with
largest sex combs

(selection)

♀ *maler* × ♂ **hybrid**

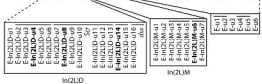
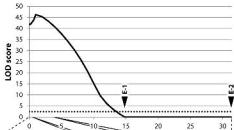
Repeat
for 36
generations

B



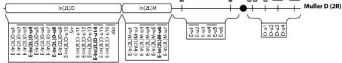
A

Muller E (2L)

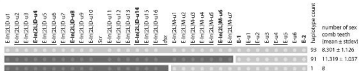


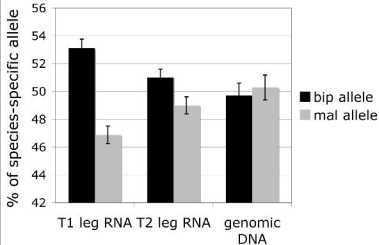
B

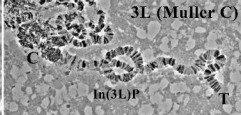
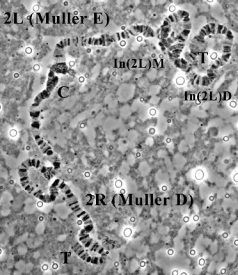
Muller B (2L)

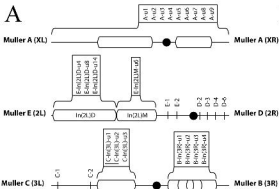


C









- markers on same genomic scaffold
- inversions
- centromeres
- markers localized by recombination mapping
- markers with uncertain relative positions

